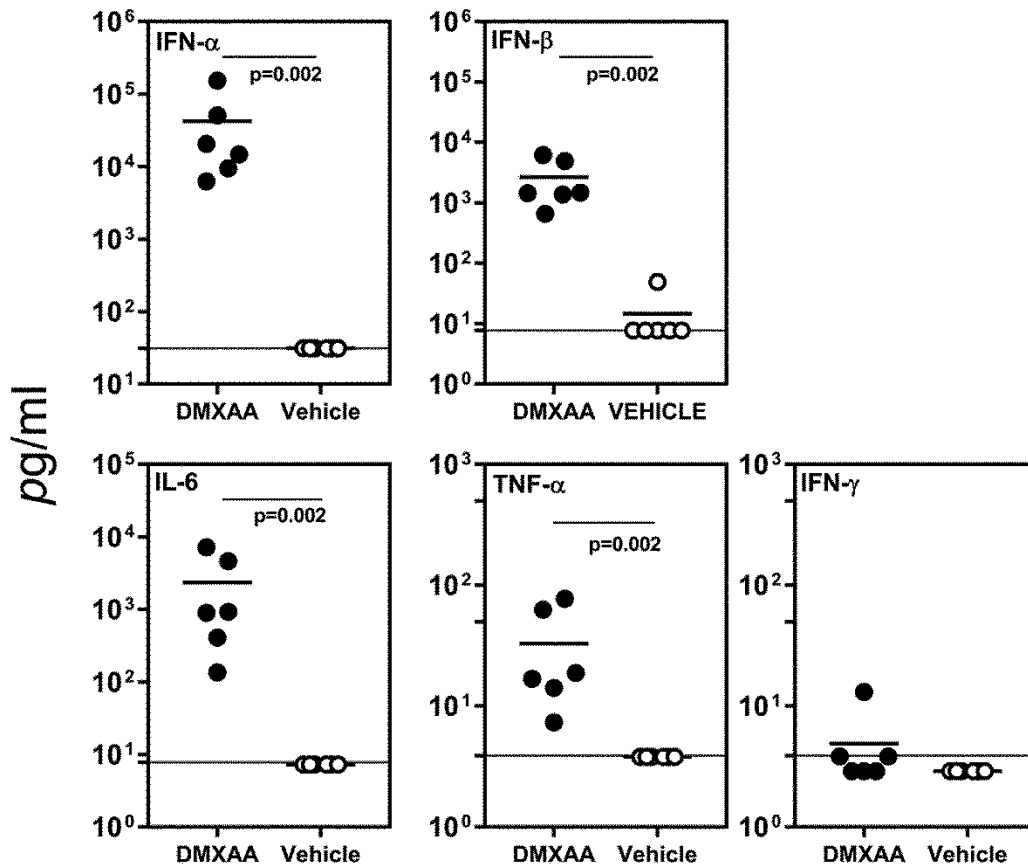


## Activation of Stimulator of Interferon Genes (STING) and Sjögren Syndrome

J. Papinska, H. Bagavant, G.B. Gmyrek, M. Sroka, S. Tummala, K.A. Fitzgerald, and U.S.

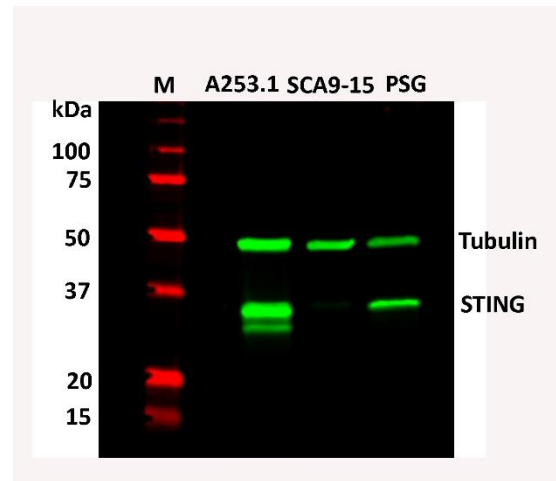
Deshmukh

### Appendix

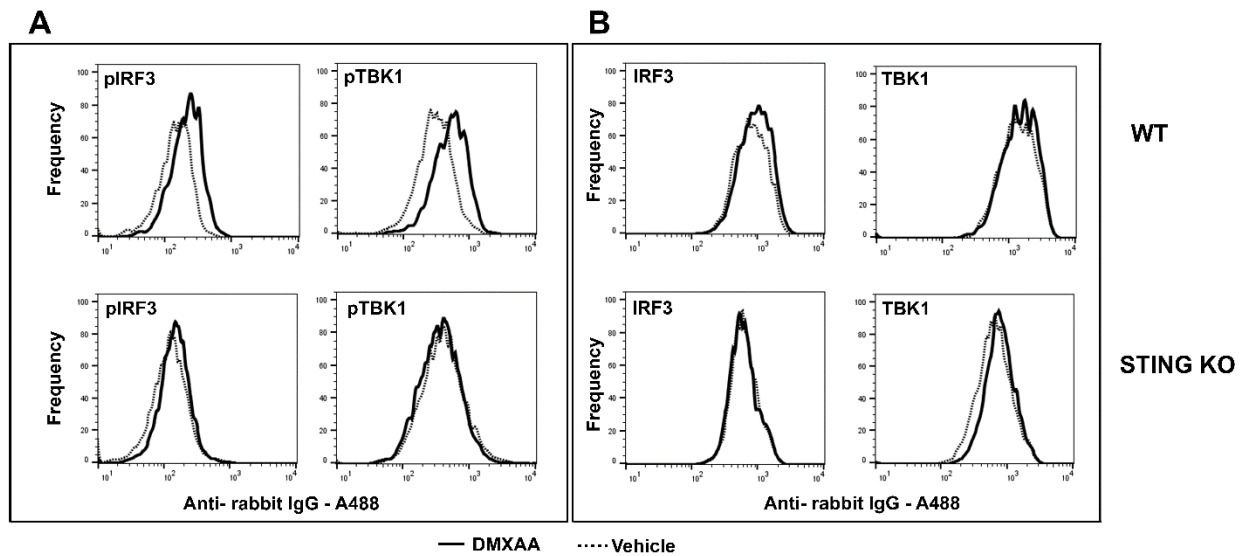


**Appendix Figure 1.** *In vivo* systemic effects of DMXAA treatment on C57BL/6 mice. The levels of circulating IFN- $\alpha$ , IFN- $\beta$ , IL-6, TNF- $\alpha$  and IFN- $\gamma$  were measured in sera obtained from mice four hours after DMXAA and vehicle treatment. The horizontal line within each graph represents the limit of detection for each of the analytes. Statistical significance was determined by two-tailed Mann-Whitney test and a  $p < 0.05$  was considered significant.

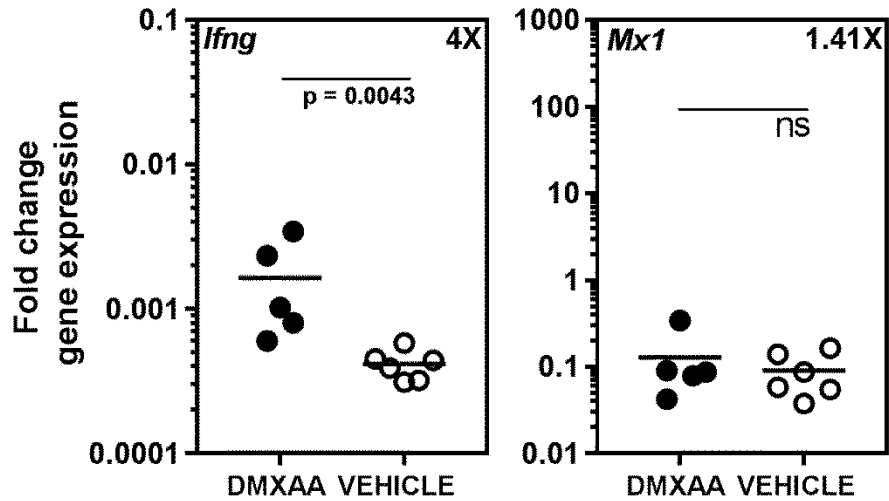
Cell line	Cell type
A253.1	Human salivary gland cell line
SCA9_15	Murine salivary gland cell line
PSG	Murine primary salivary gland cells



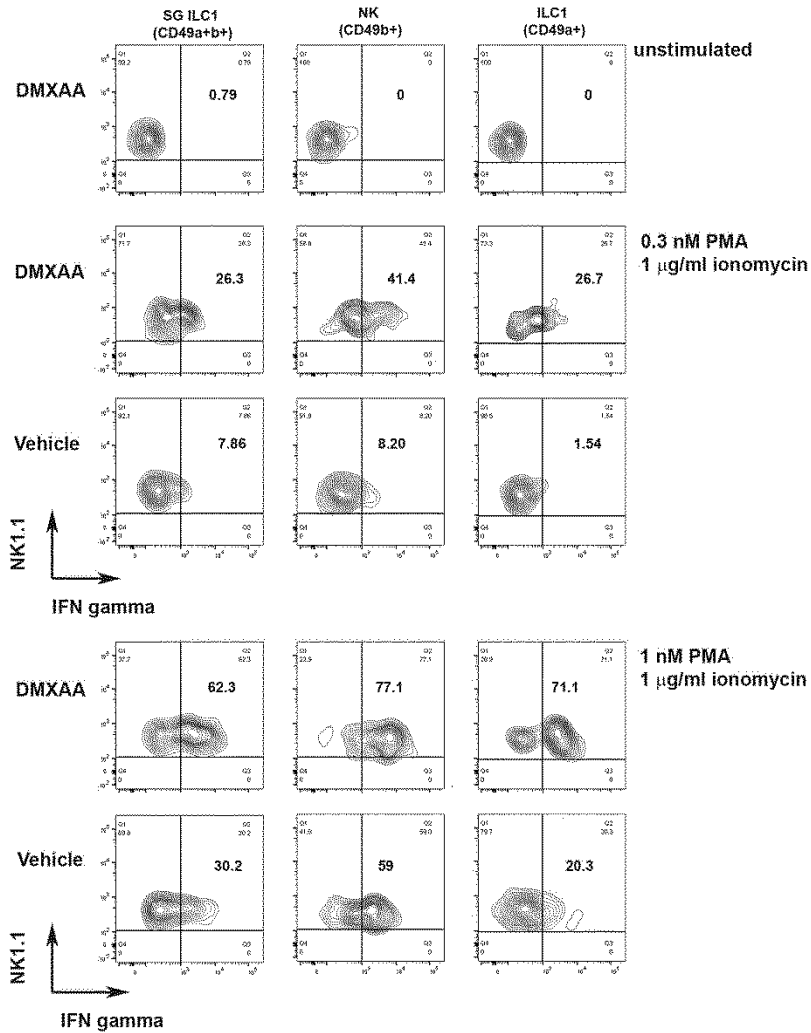
**Appendix Figure 2. STING expression in SG cells.** STING expression in different SG cell lines was analyzed by western blots. A253.1 (human) and SCA9-15 (murine) are immortalized cells. PSG: primary SG cells at passage 2. Representative image from one out of three western blots is shown. Rabbit anti-STING (D2P2F) and rabbit anti- $\alpha/\beta$ -tubulin antibodies (Cell Signaling Technology, Danvers, MA, USA) were used to probe the blots. IR dye 800-conjugated goat-anti-rabbit IgG (LI-COR, Lincoln, NB) was used to detect bound antibodies. Images were acquired using the Odyssey Classic scanner (LI-COR, Lincoln, NB).



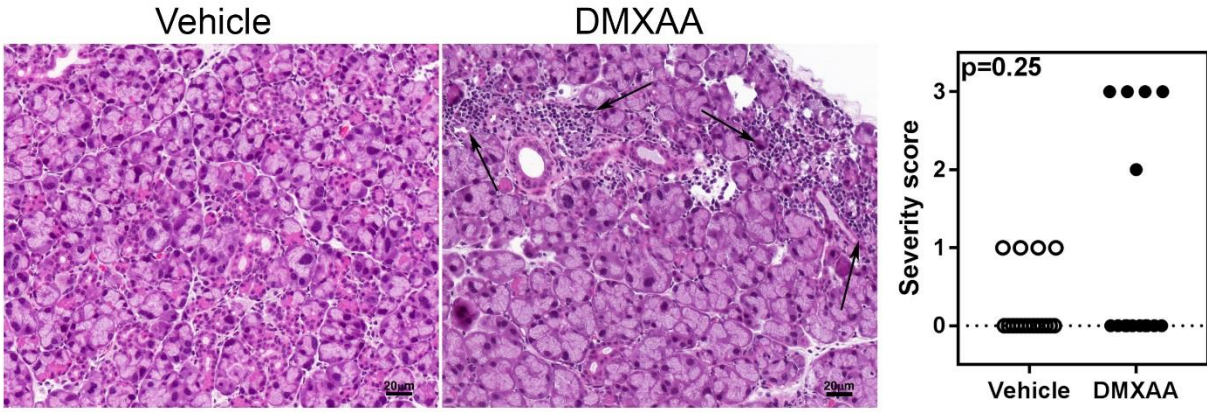
**Appendix Figure 3. DMXAA activates the STING-TBK1-IRF3 axis in primary salivary glands cells.** (A): Expression of phosphorylated IRF3 and TBK1 in wild type (WT) and STING<sup>-/-</sup> (KO) primary salivary gland cells was analyzed one hour after DMXAA treatment by flow cytometry. A consistent increase in pIRF3 and pTBK1 staining were seen in DMXAA-treated cells from WT mice in 3 independent experiments. These shifts were not evident in cells from STING KO mice. (B): The expression of TBK1 and IRF3 was not different between vehicle and DMXAA-treated cells. Cells were stained with rabbit polyclonal antibodies to pIRF3, pTBK1, IRF3 and TBK1 (Cell Signaling Technology, MA, USA) followed by Alexafluor 488 conjugated anti-rabbit IgG using standard protocols.



**Appendix Figure 4. Upregulated *Ifng* expression is seen in submandibular glands of mice, even 3 days after DMXAA treatment.** Real-time PCR analysis of gene expression in submandibular SG from DMXAA-treated group shows significant upregulation in the expression of *Ifng* but not *Mx1*. The numbers in the right corner show mean fold increase in expression level in DMXAA-treated mice over vehicle treated mice. Statistical significance was determined by two-tailed Mann-Whitney test and a  $p < 0.05$  was considered significant.

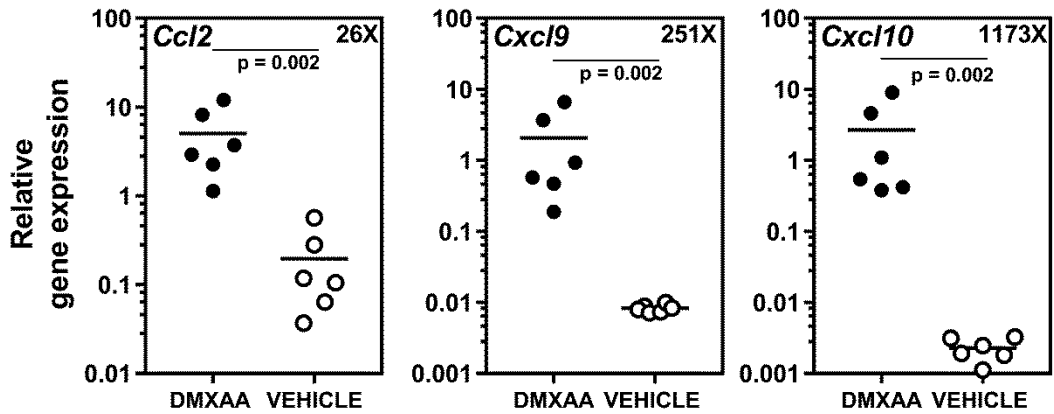


**Appendix Figure 5. IFN- $\gamma$  production by SG ILC1s in DMXAA treated mice.** Submandibular glands from mice (2 per group) injected with either DMXAA or vehicle were harvested 6 h after treatment. Single cell suspensions from each group were pooled and stimulated with PMA (0.3 nM or 1 nM) and Ionomycin (1  $\mu$ g/mL) for 6 h in the presence of Brefeldin A. Cells were stained with the panel of antibodies for surface markers to identify NK cells and ILC1, followed by staining for intracellular IFN- $\gamma$  using standard protocols. Data was acquired on a LSR II machine under FACSDiva software and data was analyzed with FlowJo software. Results are a representative of two independent experiments.

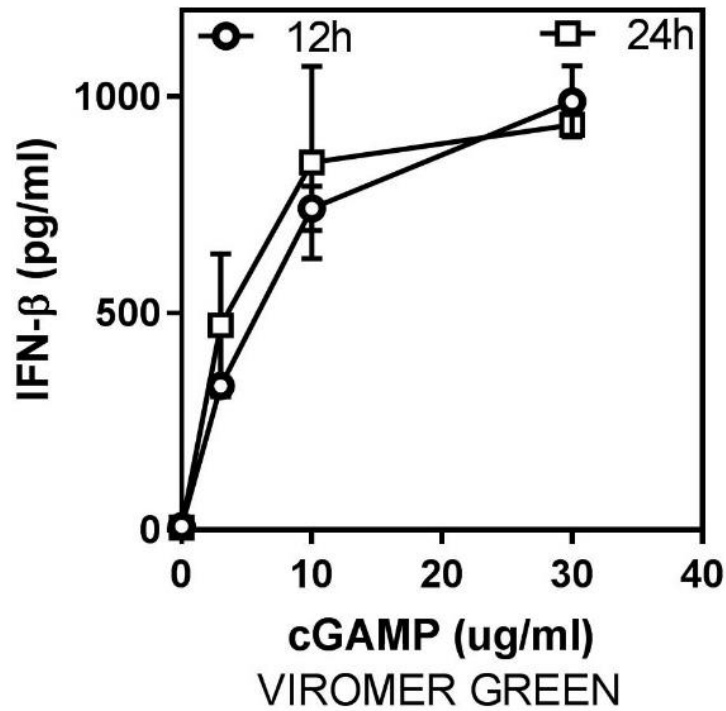


**Appendix Figure 6. Higher trend of lacrimal gland inflammation in DMXAA treated mice.**

Representative images of H&E stained sections of formalin-fixed and paraffin-embedded lacrimal glands from either vehicle (left panel) or DMXAA treated (right panel) mice. **B.** Severity of inflammation in lacrimal glands obtained from mice euthanized between 1-2 months post-treatment was scored by an observer blinded to experimental details. Two-tailed, Mann-Whitney test was used to determine the statistical significance.

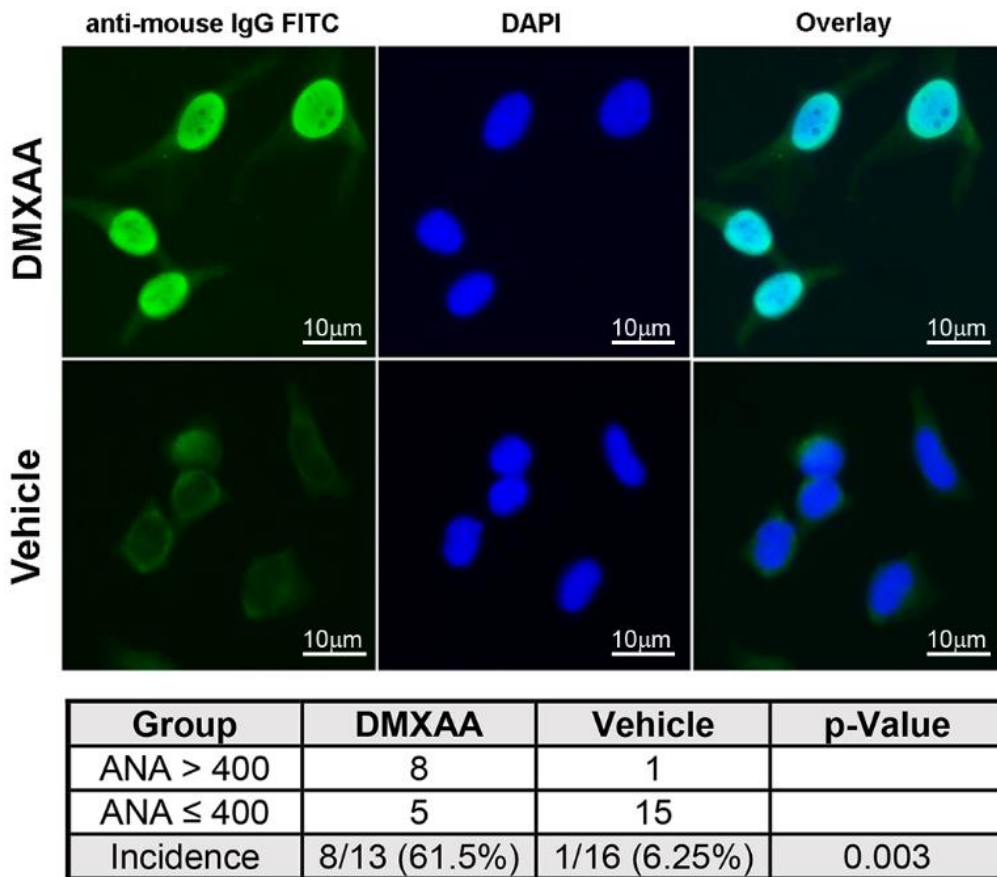


**Appendix Figure 7. Upregulated expression of IFN-dependent chemokines in SG of DMXAA treated mice.** Real-time PCR analysis of gene expression in submandibular SG from DMXAA-treated group shows significant upregulation in the expression of *Ccl2*, *Cxcl9*, and *Cxcl10*. The numbers in the right corner show mean fold increase in expression level in DMXAA treated mice over vehicle treated mice. Statistical significance was determined by two-tailed Mann-Whitney test and a  $p < 0.05$  was considered significant.



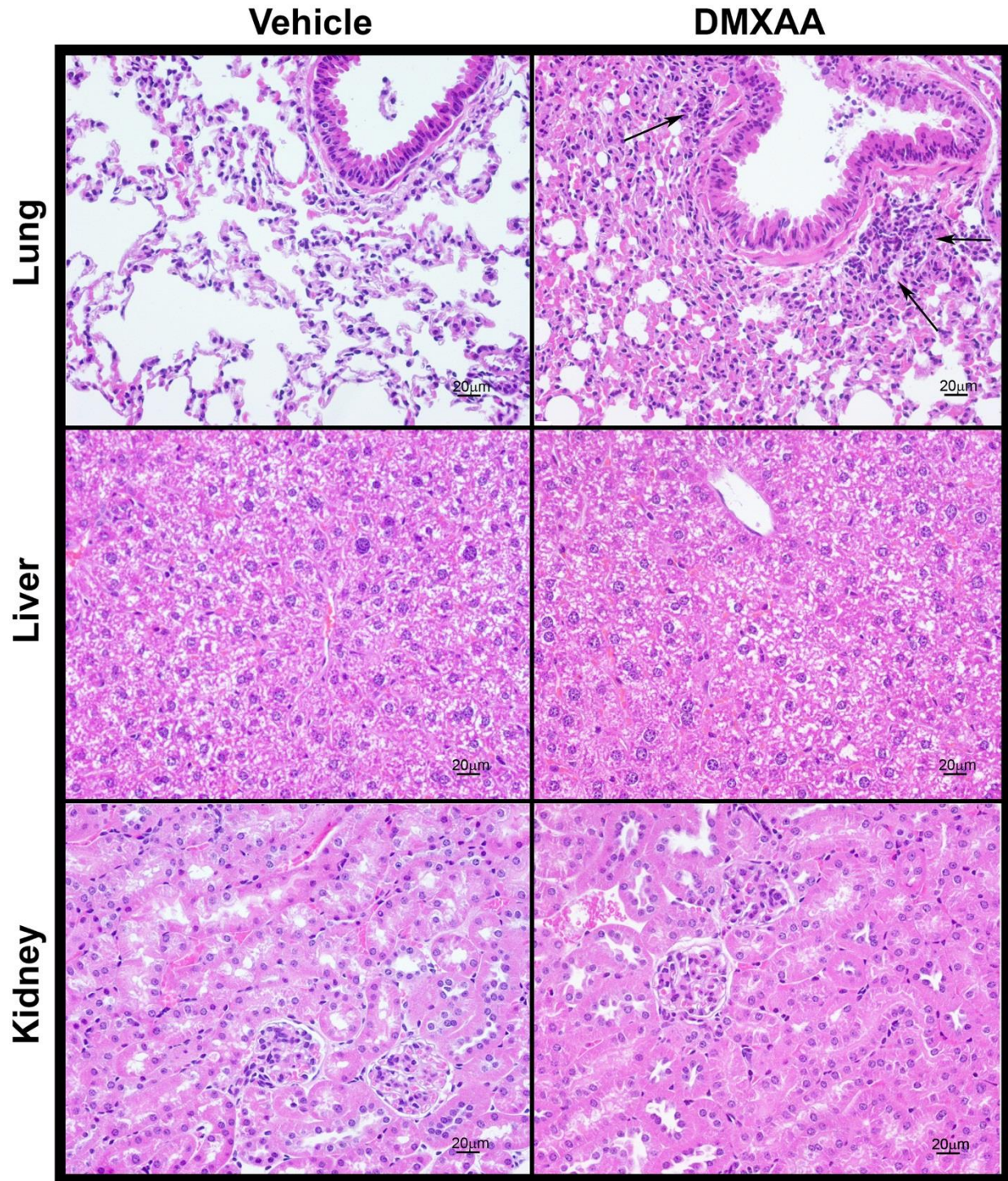
**Appendix Figure 8. Primary salivary gland cells produce IFN- $\beta$  in response to canonical STING ligand 2'3'-cGAMP.** Primary salivary gland cells were transfected with different concentrations of 2'3'-cGAMP (InVivoGen, San Diego, CA) using transfection reagent Viromer Green (Origene, Rockville, MD), by following manufacturer's instructions. IFN- $\beta$  present in culture supernatants obtained at 12 h and 24 h was estimated by ELISA.





**Appendix Figure 9. DMXAA treatment induces high titer of anti-nuclear antibodies (ANA).**

Sera from mice treated with either DMXAA or vehicle were obtained at euthanasia (1-2 months after first treatment), and endpoint ANA titers were determined. HeLa cells grown on coverslips were fixed with methanol and used as substrate. Bound antibodies were detected by FITC-labeled goat anti-mouse IgG (Green). Nuclei (Blue) were stained with DAPI. The **top panel** shows representative ANA staining pictures. The **bottom panel** shows that the frequency of mice with high titer (>400) of ANA was significantly higher (p=0.003) in the DMXAA group. Two-tailed Fisher’s exact test was used to determine the statistical significance.



**Appendix Figure 10. Only lungs from DMXAA treated mice show presence of inflammatory cell infiltrates.** Sections of paraffin-embedded lung, liver and kidney from vehicle and DMXAA treated mice were stained with H&E and evaluated for the presence of cellular infiltrates.

Representative images for each tissue are shown. Lungs showed peri-bronchial inflammatory infiltrates (indicated by arrows) as well as parenchymal involvement. Inflammatory cell infiltrates were not detected in pancreas.

**Appendix Table. List of antibodies used for ILC1 staining.**

<b>Name of antibody</b>	<b>Clone</b>	<b>Fluorophore</b>	<b>Manufacturer</b>
Anti-mouse CD3 $\epsilon$	145-2C11	PE	eBioscience
Anti-mouse CD5	53-7.3	PE	eBioscience
Anti-mouse CD19	eBioID3	PE	eBioscience
Anti-mouse TCR $\gamma\delta$	eBioGL3	PE	eBioscience
Anti-mouse TCR $\beta$	H57-597	PE	BD Biosciences
Anti-mouse Fc $\epsilon$ RI	MAR-1	PE	eBioscience
Anti-mouse CD8 $\alpha$	53-6.7	PE	eBioscience
Anti-mouse CD4	RM4-5	PE-Cy5	BD Biosciences
Anti-mouse Thy1.2 (CD90.2)	30-H12	PE-Cy7	eBioscience
Anti-mouse NK1.1	PK136	AlexaFluor780	eBioscience
Anti-mouse CD49a	Ha31/8	PerCp-Cy5.5	BD Biosciences
Anti-mouse CD49b	DX5	BV421	Biolegend
Anti-mouse CD45	30-F11	BV605	eBioscience
Anti-mouse IFN $\gamma$	XMG1.2	AlexaFluor647	Biolegend